



Impacts of elevated $p\text{CO}_2$ on estuarine phytoplankton biomass and community structure in two biogeochemically distinct systems in Louisiana, USA

Amy J. Mallozzi^a, Reagan M. Errera^{b,*}, Sibel Bargu^a, Achim D. Herrmann^c

^a Louisiana State University, Department of Oceanography and Coastal Science, 1002-Q Energy, Coast and Environment Building, Baton Rouge, Louisiana 70803, United States

^b Louisiana State University, School of Renewable Natural Resources, 227 Renewable Natural Resource Building, Baton Rouge, Louisiana 70803, United States

^c Louisiana State University, Department of Geology and Geophysics and Coastal Studies Institute, E235 Howe Russell Kniffen, Baton Rouge, Louisiana 70803, United States

ARTICLE INFO

Keywords:

Coastal acidification
CHEMTAX
Long-term incubation
pH
Carbonate chemistry
C:N

ABSTRACT

Ocean acidification has the potential to impact the ocean's biogeochemical cycles and food web dynamics, with phytoplankton in the distinctive position to profoundly influence both, as individual phytoplankton species play unique roles in energy flow and element cycling. Previous studies have focused on short-term exposure of monocultures to low pH, but do not reflect the competitive dynamics within natural phytoplankton communities. This study explores the use of experimental microcosms to expose phytoplankton assemblages to elevated $p\text{CO}_2$ for an extended period of time. Phytoplankton communities were collected from two biogeochemically distinct Louisiana estuaries, Caillou Lake (CL) and Barataria Bay (BB), and cultured in lab for 16 weeks while bubbling CO_2 enriched air corresponding to current (400 ppm) and future (1000 ppm) $p\text{CO}_2$ levels. Results suggest that elevated $p\text{CO}_2$ does not implicitly catalyze an increase in phytoplankton biomass (chlorophyll *a*). While pigment data showcased a parabolic trend and microscopic observations revealed a loss in species diversity within each major taxonomic class. By the end of the 16-week incubation, 10 out of the 12 cultures had a community structure analogous to that of the startup phytoplankton assemblage collected from the field. Natural phytoplankton assemblages exposed to elevated $p\text{CO}_2$ experienced multiple transitional states over the course of a 16-week incubation, indicating that there is no deterministic successional pathway dictated by coastal acidification but community adaptation was observed.

1. Introduction

Unprecedented climatic changes brought about by the rise of large-scale conventional energy production have spurred a host of studies concerning ecosystem changes. Prior to the industrial revolution, the atmospheric concentration of greenhouse gas carbon dioxide had not exceeded 300 ppm for the last 15 million years (Pearson and Palmer, 2000). Anthropogenic activities, such as combustion of fossil fuel and deforestation, have increased modern $p\text{CO}_2$ levels to 400 ppm (Monastersky, 2013). The Intergovernmental Panel on Climate Change (IPCC) predicts levels could rise to 1000 ppm by the end of the 21st century if business continues as usual (Solomon et al., 2007). About 30% of atmospheric CO_2 enters the oceans altering the balance of inorganic carbonate chemistry (Sabine et al., 2004). Increasing CO_2 in the ocean reacts with H_2O to form carbonic acid (H_2CO_3), which releases

hydrogen ions (H^+) as it further dissociates. Excess H^+ lowers the pH of the water, making it more acidic. By 2100, ocean acidification could drop the pH of the ocean by 0.4 units (Caldeira and Wickett, 2003).

Acidification has been well studied in the open-ocean (Feely et al., 2004; Orr et al., 2005; Riebesell and Tortell, 2011), but less work has been done in near-shore systems because of its complexity. Changes in seawater inorganic carbonate chemistry will not be uniform around the globe, as regional factors can have a larger impact on local water chemistry variability than global $p\text{CO}_2$ increases (Wanninkhof et al., 2015). In neritic zones, pH varies as a function of salinity, alkalinity, nutrient input, production, respiration, calcification, and degradation of organic matter. In such a dynamic environment, it becomes a challenge to pinpoint a suitable reference point from which the ecosystem deviates, so the local manifestation of increased $p\text{CO}_2$ is unknown. River input has a direct influence on salinity and nutrients, but changes

* Corresponding author.

E-mail addresses: rerrera@lsu.edu (R.M. Errera), sbargu@lsu.edu (S. Bargu), aherrmann@lsu.edu (A.D. Herrmann).

<https://doi.org/10.1016/j.jembe.2018.09.008>

Received 1 June 2018; Received in revised form 27 September 2018; Accepted 28 September 2018

Available online 18 November 2018

0022-0981/ © 2018 Published by Elsevier B.V.

in accordance with rainfall, land use, and river diversions. Furthermore, physical and biological drivers often have oppositional effects of either compounding or mitigating acidification.

Estuaries are highly productive environments in which phytoplankton blooms can be triggered by excessive nutrients. Photosynthetic activity creates a sink for CO₂, with resonating effect on the inorganic carbonate chemistry of the water (Dai et al., 2008). In the Gulf of Mexico, algal blooms have been correlated with increased drawdown of DIC and increased pH (Lohrenz and Cai, 2006). In Louisiana, the biological uptake of inorganic carbon in surface waters and subsequent downward flux is among the highest in the world (Cai, 2003). However, the production-sequestration model may be too simplistic, as eutrophication may indirectly accelerate acidification. Following algal die-off, microbial respiration increases and releases CO₂ as a waste product, decreasing pH (Cai et al., 2011; Wallace et al., 2014). Some models demonstrate that anthropogenic CO₂ emissions plus CO₂ from respiration facilitate acidification in a more than additive fashion, particularly at higher temperatures (Sunda and Cai, 2012). Others studies show just the opposite, that eutrophication in coastal areas will offset pH depression and ultimately play a more significant role in carbonate chemistry of coastal zones than ocean acidification (Borges and Gypens, 2010).

Coastal Louisiana is an ideal example of a mixing zone in constant physiochemical fluctuation due to high river input. Louisiana's large-river deltaic estuaries receive 55% of freshwater inflow from the Atchafalaya River in the west and the Mississippi River in the east (Bianchi et al., 1999). In these locations, estuarine carbonate chemistry doesn't vary linearly with salinity, and thus is not a simple additive function of freshwater and seawater components (Keul et al., 2010). In most freshwater systems alkalinity is low, due to a relative deficit of bicarbonate and other ions, so estuaries generally have a weaker buffering capacity than oceanic environments (Cai, 2003). However, the northern Gulf of Mexico river-plume represents one of the most highly buffered areas in the United States (Wang et al., 2013), due to high concentrations of bicarbonate delivered by the Mississippi (TA 2400 μmol kg⁻¹) and the Atchafalaya (TA 2000 μmol kg⁻¹) (Cai et al., 2010). Total alkalinity increases approaching the mouth of the Mississippi (Keul et al., 2010), but local buffering capacity may also be linked to the biological removal of CO₂.

Phytoplankton dynamics are key in understanding how increased pCO₂ will affect biogeochemical cycling. Collectively, these producers not only sequester carbon to the deep ocean but also supply energy to higher trophic levels. Changes in phytoplankton communities will change taxon-specific nutrient cycling (Tagliabue et al., 2011) and have a corresponding impact on their role as carbon sinks. There is a general assumption that primary productivity will increase with more available carbon, but whether the effect on marine production will be positive or negative is uncertain (Hein and Sand-Jensen, 1997; Schippers et al., 2004; Beardall et al., 2009; Taucher and Oschlies, 2011; Guo et al., 2012; Grear et al., 2017). Furthermore, increased biomass alone is not inclusive of the functional changes brought about by shifts in phytoplankton community composition. Acidification may cause a shift towards less nutritious species or degrade the nutrition potential of an existing species (Rossoll et al., 2012), with resonating effects up the food web (Hettinger et al., 2013).

Individual species of phytoplankton will be uniquely affected by acidification, largely due to regulation of their carbon concentrating mechanisms (CCM) (Collins et al., 2014). For this reason, much of the literature illustrates a bidirectional reaction to acidification across and within taxa. For example, Rost et al. (2008) reports contradictory results within the major plankton functional types (PFTs): silicifiers (diatoms), calcifiers (coccolithophores), and diazotrops (cyanobacteria). The response of individual phytoplankton species does not capture the dynamics within natural phytoplankton communities, as natural phytoplankton communities are comprised of a diversity of species, each varying in physiology and potential for adaptation.

Competition within and across groups is also likely to be affected by elevated pCO₂ (Dutkiewicz et al., 2015).

Investigations of community response to ocean acidification have been limited yet have the highest potential for global application. Some offer evidence that increased pCO₂ could significantly alter physiology and community structure (Eggers et al., 2014; Tortell et al., 2002; Tortell et al., 2008). Tortell et al. (2002, 2008) observed a shift from dinoflagellates to larger diatoms and overall increase in productivity. Results from Eggers et al. (2014) also indicated a move towards dominance of large diatoms. However, within a phytoplankton community Kim et al. (2006) saw an increase in only a singular diatom species *Skeletonema costatum*, and Nielsen et al. (2010, 2012) found no difference between succession in treated versus untreated assemblages. Natural communities from Narragansett Bay also indicated shifts in community composition at different pCO₂ concentrations, but in contrast to Tortell et al. (2002, 2008), noted an increase in small (< 5 μm) phytoplankton growth rates at elevated pCO₂ conditions suggesting a shift in the overall size distribution of the community (Grear et al., 2017). This could be due to the origin of the initial community and highlights the need for site specific studies.

Previous community studies were short-term, terminating after two weeks, relying on fast turnover to supply a quick, sufficient model of succession using batch culturing techniques (Tortell et al., 2002; Nielsen et al., 2012; Grear et al., 2017). Long-term community level experiments are essential to address how ocean acidification and community adaptation occur on the same timescale (Raven et al., 2005; Rost et al., 2008). Prolonged temporal scales ensure the biotic response reflects recovery, adaptation and ecosystem resilience. Through highly applicable, long-term bulk microcosms can differ from natural systems under prolonged conditions (French and Watts, 1989) due to culturing effects. Semi-continuous microcosms culturing techniques have been noted to be useful in prolonging experimental conditions (Kranz et al., 2009; Tortell et al., 2008; LaRoche et al., 2011) and have been shown to minimize the effects of long-term culturing thus providing an additional tool to explore community adaptation. This study seeks to further our understanding of phytoplankton response to elevated pCO₂ in estuarine systems, and the biogeochemical and trophic implications using community-level experiments, long-term acclimation techniques and plankton communities' specific to freshwater dominated estuaries in the southeast United States. The structure of local phytoplankton communities is a mutable function of the in situ environmental conditions (Wissel et al., 2005); thus different communities can be expected in different areas.

2. Materials and methods

2.1. Site selection and field sampling

In fall 2016, natural water samples and phytoplankton communities were collected from two sites within southern Louisiana (Fig. 1), which provided naturally distinct habitats in terms of salinity and nutrient levels. Caillou Lake (29.241100, -90.935333) is influenced seasonally by the Atchafalaya River and has greater freshwater input. While lower Barataria Bay (29.271700, -89.963083) is represented by poor water quality (e.g., dissolved organics) during high river discharge and runoff. This site experiences overall reduced freshwater input and increasing salinities.

Water quality data was collected in the field at the time of sampling. Temperature (°C) and salinity were recorded using a pre-calibrated YSI (Yellow Springs Instrument) Model 85 deployed at 1 m below the sea surface. Water clarity was measured by Secchi disc. To quantify in situ inorganic carbon, dissolved inorganic carbon (DIC) and total alkalinity (TA) samples were collected in the field, poisoned with 0.02% mercuric chloride (HgCl₂) according to Dickson et al. (2007), placed on ice for transportation, and stored at 4 °C until analysis. Additionally, whole water subsamples of 200 mL were collected for microscopic analysis,

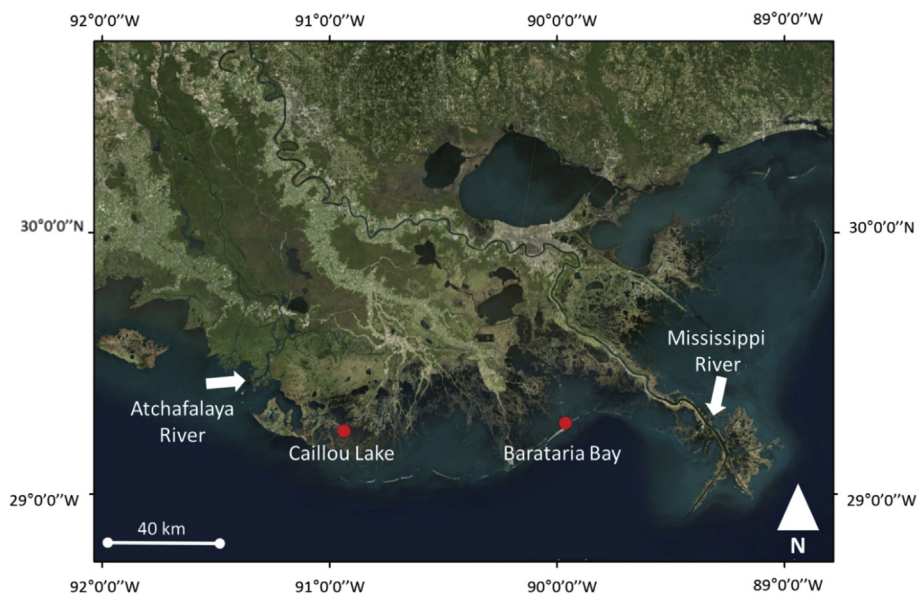


Fig. 1. Collection sites in Caillou Lake and Barataria Bay (red circles). Arrows indicate respective freshwater sources which influence each estuarine ecosystems. (For interpretation of the references to colour in this figure legend, the reader is referred to the web version of this article.)

preserved in the field with 2% glutaraldehyde, transported on ice, and stored at 4 °C.

Seawater was filtered in the field through an 80 µm pore size mesh screen into 22-L Nalgene carboys, capped with no headspace and covered for transportation back to Baton Rouge, LA (approximately 3-h drive from each location). Removal of large heterotrophic plankton was necessary to limit the impact of long-term bottle effects (Sommer, 1985). Upon return to laboratory facilities, water was mixed and distributed in triplicate based on $p\text{CO}_2$ treatment and site among 25-L glass carboys, each replicate contained 20-L of estuarine water. All additional sampling (for micronutrients, trace metals, chlorophyll *a*, photopigments, and CHN) was conducted after transportation to Louisiana State University (LSU). Collection at the two sites occurred within 48-h of each other.

2.2. Semi-continuous microcosm treatments

Both sites were treated with two different $p\text{CO}_2$ levels; a control of [400] ppm and elevated level of [1000] ppm. Placement of each treatment vessel was randomized within the incubation location. Phytoplankton were grown under a 12 h:12 h light:dark cycle using daylight fluorescent bulbs (5000 Kelvin, CRI 82, 2150 lm brightness). Photosynthetically available radiation (PAR) was measured with Biospherical Instruments' Quantum Scalar Laboratory (QSL) sensor Model 2100 and varied between 40 and 50 µmol quanta $\text{m}^{-2} \text{s}^{-1}$ in each treatment. Temperature, as measured with a dual pH/temperature probe, ranged between 20 and 22 °C.

Inorganic carbonate chemistry was manipulated by gently bubbling humidified $p\text{CO}_2$ enriched air through fine glass frits suspended 1 cm above the bottom of the glass carboys. Treatments were gently mixed at the bottom of the culturing vessel at approximately 200 rpm of using a 2 cm stir bar to minimize growth on culturing vessel walls and cell sedimentation. High turbulence has been noted to bias growth of certain phytoplankton groups, notable dinoflagellates (Juhl and Latz, 2002), cyanobacteria (Xiao et al., 2016), and green alga (Hondzo and Lyn, 1999). While other studies indicate that these phytoplankton groups utilize turbulence to increase fitness (Sullivan et al., 2003; Sengupta et al., 2017). Turbulence remained low (200 rpm) during our experiments thus limiting the potential impact on these species. Working class certified mixture represented present-day conditions of CO_2 at [400] ppm and predicted values by 2100 of CO_2 at [1000] ppm

(IPCC, 2013). Gas flow rate was set using mass flow controllers and adjusted by rotameters per treatment at approximately 10 mL min^{-1} .

2.3. Sample collection

Sampling and nutrient additions occurred every 2 weeks. Directly following each sampling, a total of 10% of the water was removed and replaced with water from each respective field site that had been filtered (0.2 µm), autoclaved, and nutrients added to achieve an f/40 concentration. To maintain a semi-continuous culture, a 1:10 dilution was established to maintain the presence of rare species, ensure the dilution ratio did not influence community dynamics, and that the inorganic carbon within the system was not drastically altered during the dilution period (Haukka et al., 2006). Incubation occurred for a total of 16 weeks.

Dissolved inorganic carbon was collected at the start of the incubation and at experiment termination. Total alkalinity (TA) and pH measurements were taken every two weeks to monitor carbonate chemistry, and chl *a* was measured to quantify the overall algal biomass. Pigment samples were taken to examine taxonomic succession, while CHN samples were taken to measure changes in total nutritional value of the assemblage every 4 weeks. Additionally, pigment samples were taken prior to the first nutrient addition and water replacement (at day 0, 2, 7 and 16 for Caillou Lake and day 0, 4, 9, and 18 for Barataria Bay) to quantify the initial response.

2.4. Laboratory analysis

2.4.1. Chemical analysis

Dissolved inorganic nitrogen (DIN), phosphorus (DIP), and silicate (DSi) were measured by filtering 30 mL through 0.45 µm acetate membrane filters into 30 mL acid-washed high-density polyethylene bottles, which were frozen at -20 °C. Water samples were then analyzed for dissolved inorganic nutrients colorimetrically using an automated discrete analyzer (AQII; Seal Analytical). The DIN pool is comprised of $\text{NH}_4\text{-N}$ and $\text{NO}_3^- + \text{NO}_2^-$ (abbreviated as $\text{NO}_x\text{-N}$). $\text{NH}_4\text{-N}$ was measured according to EPA Method 350.1 (O'Dell, 1993a), $\text{NO}_x\text{-N}$ measured according to EPA Method 353.2 (O'Dell, 1993b), and DIP (PO_4) measured according to EPA Method 365.1 (O'Dell, 1993c). DSi concentrations were quantified on filtered subsamples using an O.I. Analytical Flow Solutions IV Autoanalyzer (APHA Method 4500-SiO₂).

Total N and total P concentrations were measured per D'Elia (1977) and USEPA Method 365.2. Pre-combusted 250 mL borosilicate BOD bottles were filled directly in water at a depth of 0.5 m at each field location to determine in-situ DIC. Dissolved inorganic carbon samples collected at the end of the incubation period (week 16) were extracted from culturing units via a peristaltic pump as detailed in Bockmon and Dickson (2014). The bottles were immediately poisoned with 0.02% super saturated HgCl_2 solution and stored at 4 °C until analysis. Samples were processed by the National Ocean Sciences Accelerator Mass Spectrometry Facility at Woods Hole Oceanographic Institution. Dissolved inorganic carbon concentrations were measured by sample acidification followed by coulometric titration (DIC Model 5011 Coulometer) (DOE, 1994; Dickson et al., 2007).

Alkalinity was measured using a modified procedure based on Dickson et al. (2007). Temperature, pH, and electromotive force (e.m.f) were measured using Thermo Electron Corporation Orion 370 pH/Ion meter. Using a Schott Titroline easy, samples were titrated with 0.097 N hydrochloric acid (HCl) to achieve a pH of 3.5, allowed to de-gas for 3 min, then titrated step-wise at 20 s intervals in 0.05 mL increments until pH 3.0, creating a Gran Line. The final value for TA was converted from potentiometric data using the SeaCarb program (<http://CRAN.R-project.org/package=seacarb>) in RStudio (<http://www.rstudio.com/>). Certified reference material (University of California, San Diego, Scripps Institution of Oceanography, CRM batch #158) was used to validate each analytic session.

A Mettler-Toledo S220 SevenCompact pH/Ion meter fitted with a InLab Reach Pro-225 pH electrode with temperature and reference probe was used to measure pH (total scale). The meter was calibrated before each sampling date using 3-points, the 4.01, 7, and 10.01 standards from Orion Application Solution. Additionally, two organic buffer solutions, Tris (2-amino-2-hydroxymethyl-1,3-propanediol) and Amp (2-aminopyridine), were prepared in artificial seawater of 15 psu according to Dickson (2007). Measurement of these standards was used to verify the probe's accuracy at the beginning of the experiment.

Particulate total carbon and nitrogen was collected and analyzed via a Costech 4010 Elemental Combustion Analyzer according to EPA method 440 (Zimmermann et al., 1997). Briefly, samples were filtered using pre-combusted glass filtration units on to pre-combusted 25 mm GF/F filters. Filters were dried overnight at 60 °C, weighed and then stored in a desiccator until analysis. All other carbonate system parameters were calculated using the CO2SYS Excel program (<http://cdiac.ornl.gov/ftp/co2sys/>) adapted by Pierrot et al. (2006) using dissociation constants from Mehrbach et al. (1973), refit by Dickson and Millero (1987), Dickson (1990), and Uppström (1974).

2.4.2. Biological analysis

Total phytoplankton biomass was determined via chlorophyll (chl) *a*. Fluorescence was measured before and after acidification with HCl using Turner fluorometer 10-AU in low light according to Parsons et al. (1984). Bulk phytoplankton groups were identified using signature pigments ratios. Identification of diagnostic pigments was identified through High Performance Liquid Chromatography (HPLC) following Pinckney et al. (1998) at the HPLC Photopigment Analysis Facility at University of South Carolina. Briefly, filters containing photopigments were lyophilized and extracted in 90% acetone and stored in the dark for 18–20 hours at –20 °C. Extracts were filtered through 0.45 µm PTFE filter (Gelman Acrodisc) and 250 µl injected into an HPLC system equipped with two reverse-phase C18 columns in series (Rainin Microsorb-MV, 0.46 × 10 cm, 3 mm, Vydac 201TP, 0.46 × 25 cm, 5 mm). A nonlinear binary gradient, adapted from Van Heukelem et al. (1995), was used for pigment separations. Solvent A consisted of 80% methanol and 20% ammonium acetate (0.5 M adjusted to pH 7.2), and Solvent B was 80% methanol and 20% acetone. Absorption spectra and chromatograms were acquired using a Shimadzu SPD-M10av photodiode array detector, where pigment peaks were quantified at 440 nm.

The following accessory pigments were recognized: chlorophyll *a*,

chlorophyll *b*, chlorophyll *c*₃, peridinin, 19-butfucoxanthin, fucoxanthin, 19-hexfucoxanthin, neoxanthin, violaxanthin, prasinoxanthin, diadinoxanthin, alloxanthin, diatoxanthin, lutein, and zeaxanthin. The chemical taxonomy algorithm CHEMTAX V1.95 (http://gcmd.nasa.gov/records/AADC_CHEMTAX.html) was then used to calculate the relative contributions cyanobacteria, chlorophytes, cryptophytes, diatoms, and dinoflagellates to the total chl *a* abundance (Mackey et al., 1996), assuming the ratio of each accessory pigment remains constant within the assemblage from each field site. As use of region-specific pigment ratios is vital in obtaining accurate results (Lewitus et al., 2005), CHEMTAX program matrices were obtained from Zhao and Quigg (2014) and provided with final pigment matrices in supplementary material (Supplementary Table 1–5). Quimiotaxonomy (referred to as taxonomy) is reported as the percentage of the total assemblage and was grouped by field site and *p*CO₂ level during analysis.

Microscopic analysis was conducted in order to verify pigment ratios and identify the most dominant phytoplankton to the lowest possible taxonomic level. Using an Axio Observer -A1 inverted microscope (Axiovert 135, Zeiss), the abundance of diatom and cyanobacteria cells were counted on gridded Sedgewick-Rafter slides and scaled to cells L⁻¹. The biovolume of an algal type (e.g. ellipsoid) was computed using similar geometric models according to Sun and Liu (2003). Ratios were verified using the summation of the biovolumes of each type within the broad taxonomic class. Samples collected from the field, at an intermediate time point (Week 8) and at the conclusion of the incubation (Week 16) were analyzed.

2.5. Data analysis

The effect of *p*CO₂ on phytoplankton assemblages was compared between sites using several different methods. Distinct 2-way analysis of variance (ANOVA) were used to determine the effect of *p*CO₂ as a fixed factor on pH, and chl *a*. The relationship between two non-categorical variables was determined using a Pearson's correlation test. All analyses were conducted using the RStudio statistical computing software, and significance was defined as a *p* value < .05. Numbers are reported as the mean ± standard deviation. The effect of *p*CO₂ on community composition (considered as the contribution of major taxonomic groups to the total chl *a* pool, square root transformed to increase the effect of less dominant taxa) was determined using a permutational multivariate analysis of variance (PERMANOVA) in PRIMER-6 measuring Bray-Curtis Similarity. 2D multidimensional scaling (MDS) graphs were generated through PRIMER, with overlay clusters based on group-average super imposed on the plot at 60% and 80% similarity.

3. Results

Caillou Lake (CL) and Barataria Bay (BB) water clarity, inorganic chemistry, and temperature were comparable at the time of sampling (Table 1). Caillou Lake, influenced by the Atchafalaya River, had a salinity of 12 while Barataria Bay, which is influenced by the Mississippi River, had a higher salinity of 16. In both sites, the DIN ($\text{NO}_3^- + \text{NO}_2^-$) was below detection, whereas the phosphorous (PO_4) was very low but still measurable. Silica content for Caillou Lake was higher, 81.467 µM, than Barataria Bay, 44.733 µM, although the phytoplankton biomass was reversed, with higher biomass recorded in Barataria Bay ($28.62 \pm 1.32 \mu\text{g chl } a \text{ L}^{-1}$) than Caillou Lake ($10.78 \pm 0.75 \mu\text{g chl } a \text{ L}^{-1}$). The ratio of C:N in Caillou Lake, 6.98 ± 0.18 , was very close to Redfield ratio of 6.625, whereas in Barataria Bay the C:N was slightly higher at 7.06 ± 1.17 .

3.1. Field (initial) phytoplankton communities

The phytoplankton community in Caillou Lake (Fig. 2) was dominated by a diverse assemblage of cyanobacteria (81.4%), including

Table 1

Water quality parameters and diversity for Caillou Lake and Barataria Bay, Louisiana in Oct 2017. Detection limit for $N = 1.43 \mu\text{M}$, $P = .13 \mu\text{M}$. Averaged $n = 3$ unless otherwise indicated with standard deviation.

	Caillou Lake	Barataria Bay
GPS coordinates	29.241100, -90.935333	29.271700, -89.963083
Date sampled	10-2-2016	9-30-2016
Major river influence	Atchafalaya	Mississippi
Temperature ($^{\circ}\text{C}$)	26.3	29.6
Salinity	12.2	16.6
Water column depth (m)	1.8	2.6
Water clarity (m)	0.3	1
Total alkalinity ($\mu\text{mol kg}^{-1}$)	1987.65 ± 2.2	2039.34 ± 18.58
DIC ($\mu\text{mol kg}^{-1}$)	$1650, n = 1$	$1500, n = 1$
$\text{NO}_2^- + \text{NO}_3^-$ (μM)	< 1.43	< 1.43
NH_4 (μM)	4.00 ± 0.071	17.49 ± 0.00
PO_4 (μM)	0.81 ± 0.00	0.87 ± 0.00
Si (μM)	81.47 ± 1.81	44.73 ± 0.06
Chl a ($\mu\text{g L}^{-1}$)	10.78 ± 0.75	28.62 ± 1.32
C:N	6.98 ± 0.18	7.06 ± 1.17
H Diversity Index	0.72 ± 0.08	1.35 ± 0.01

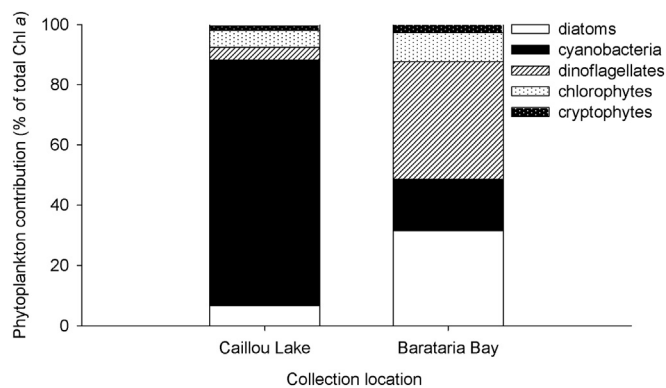


Fig. 2. Percent phytoplankton composition based on total chl a (estimated by ChemTax) in Caillou Lake and Barataria Bay. Percent contribution bars represent an average ($n = 3$) collected from the field locations.

filamentous cyanobacteria, *Microcystis* sp., *Anabaena* sp., *Raphidiopsis* c.f. *curvata*, *Cylindrospermopsis* c.f. *curvispora*, and *Cylindrospermopsis* c.f. *raciborskii*. The presence of diatoms (6.74%) was a mixture of small pennate *Navicula* sp., medium size *Cylindrotheca closterium* (also known as *Nitzschia closterium*), and *Chaetoceros* c.f. *simplex*. Few dinoflagellates of the *Ceratium* and.

Protoperdinium genus were also observed, making up 4.32% of the pigment volume (Supplementary Table 6). The nanoflagellates (7.54%) were unable to be unambiguously identified, though the pigment analysis suggests they were comprised of chlorophytes and cryptophytes.

The phytoplankton community in Barataria Bay (Fig. 2) was more diverse. Large diatoms made up 31.48% of the total assemblage, including chain-forming *Chaetoceros* sp., *Skeletonema* sp., and *Thalassionema* c.f. *nitzschoides*, as well as *Coscinodiscus* sp. and *Cylindrotheca closterium* were observed. Cyanobacteria represented only 17.07% of the community, but was a mix of filamentous cyanobacteria were observed and included chains of *Anabaena* sp., *Cylindrospermopsis* sp., *Microcystis* sp., and *Raphidiopsis* sp. Dinoflagellates (39.03%) had the most significant contribution to the pigment volume, both *Karenia mikimotoi*, and *Prorocentrum minimum* were identified (Supplementary Table 7). Chlorophytes and cryptophytes also has a substantial presence (12.41%) but were unable to be definitively identified to a lower taxonomic level. Euglenophytes were microscopically observed in field samples, though not included as a group in the pigment analysis, as they disappeared quickly after incubation began and have overlapping pigments with chlorophytes.

3.2. Long-term incubation

Within 2 weeks of incubation, pH levels begun to diverge between the two $p\text{CO}_2$ treatments and achieved a significant difference ($p > .01$) after 6 weeks of incubation (Fig. 3 A, D). The greatest pH difference was observed at 10 weeks, but by weeks 14 and 16 the pH of the cultures began to converge once more (Fig. 3 A, D), though the overall CO_2 available to the plankton community was still elevated in the [1000] $p\text{CO}_2$ treatments.

Total alkalinity (TA) remained stable, ranging between 1800 and 2000 $\mu\text{mol kg}^{-1}$ in both $p\text{CO}_2$ treatments for the first 10 weeks of the experiment (Fig. 3 B, E). Starting at week 12, CL [400] ppm treatments began to gradually decrease to 1400–1600 $\mu\text{mol kg}^{-1}$ while CL [1000] ppm cultures remained unchanged. At week 14, two replicates of the BB [400] cultures decreased significantly to 420 $\mu\text{mol kg}^{-1}$ and 975 $\mu\text{mol kg}^{-1}$, while the [1000] ppm treatments remained stable (Fig. 3 B, E). The pH of all cultures rose steadily over the course of the experiment while the total alkalinity dropped, indicating changes in carbonate chemistry may have a relationship to aging of the cultures (Fig. 3 A, D). No relationship was identified between biomass and pH.

Over the course of the incubation, CL [400] ppm cultures achieved a higher chl a ($7.05 \pm 9.10 \mu\text{g chl } a \text{ L}^{-1}$) than CL [1000] ppm ($6.87 \pm 8.97 \mu\text{g chl } a \text{ L}^{-1}$), following nutrient additions (week 4, week 10, week 16) (Fig. 3 C). Acidification treatments did not impact on BB chlorophyll, as [400] ppm treatments had an average biomass of $4.40 \pm 4.85 \mu\text{g chl } a \text{ L}^{-1}$, and [1000] ppm treatment was $4.41 \pm 4.86 \mu\text{g chl } a \text{ L}^{-1}$ (Fig. 3 F).

3.3. Phytoplankton succession

During the first two weeks of incubation, pigment samples were taken at more frequent time intervals in order to elucidate the initial response of the assemblages collected from the field to culture conditions (Fig. 4). Though a pH difference had been established by the end of the first 2 weeks of incubation (Fig. 3 A, B), there was virtually no difference in the community structure between [400] and [1000] ppm treatments in either assemblage. Between weeks 2 and 4, the response of each individual culture diverged (Figs. 5 and 6).

3.3.1 Caillou Lake

Both [400] ppm and [1000] ppm cultures had increased in diatoms and chlorophytes while decreasing in cyanobacteria by week 2 of the incubation (Fig. 4, A-B) and continued through week 4. The control CL [400] ppm replicates reached a maximum diatom dominance (84% of the phytoplankton assemblage) (Fig. 5 B, C) by week 4, while [1000] ppm replicates were more diverse, with one reaching 86% diatoms (Fig. 5 D), while the other two were at 42% diatoms and 20% diatoms (Fig. 5 E,F). Chlorophytes remained steady throughout the experiment, between 6 and 15%, with a spike in one CL [1000] ppm replicate (Fig. 5 F). Diatom peaks corresponded with C:N (Fig. 5).

After 8 weeks of incubation, the CL [400] ppm cultures were dominated by diatoms *C. closterium* (10^6 cells L^{-1}) and *Navicula* sp. (10^5 – 10^6 cells L^{-1}). Cyanobacteria was a diverse mixture of filamentous cyanobacteria (10^6 to 10^7 cells L^{-1}) and *Microcystis* sp. (10^6 cells L^{-1}). Notably, one CL [400] replicate also contained blooms of small centric diatoms (5×10^6 cells L^{-1}) and chain forming *Anabaena* sp. (3×10^6 cells L^{-1}), corresponding with a sharp spike in C:N to 10.1 (Fig. 5 B) (Supplementary Table 8). Within the CL [1000] ppm assemblages, diatoms were less dominate but the taxonomic composition was also predominately *C. closterium* (10^5 to 10^7 cells L^{-1}) and *Navicula* sp. (10^5 – 10^6 cells L^{-1}). Cyanobacteria was comprised of a filamentous species (10^6 to 10^7 cells L^{-1}) (Supplementary Table 9). C:N ranged from 6.2 to 10.1 in [400] ppm cultures and from 7.2 to 10.2 in [1000] ppm cultures.

By week 12, all CL [400] ppm cultures had rapidly decreased in

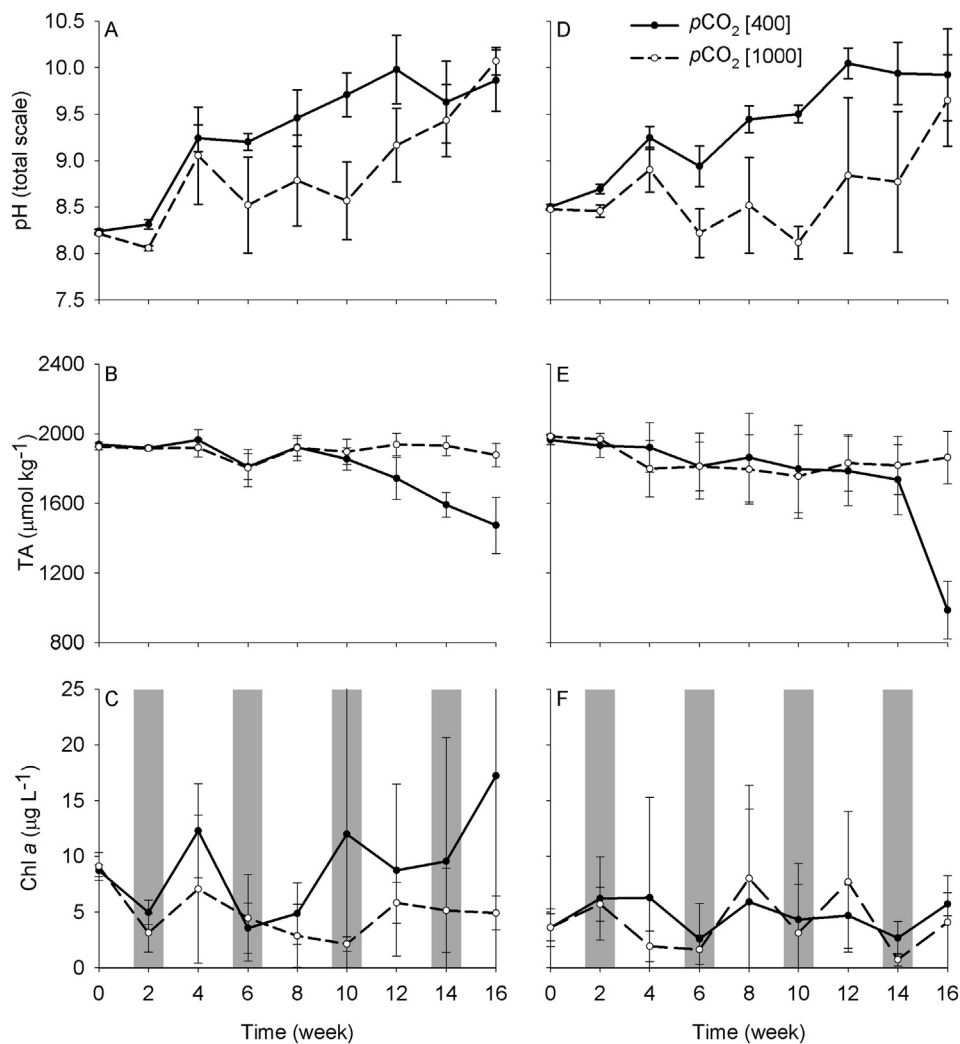


Fig. 3. Mean pH (A, D), total alkalinity (B, E), and biomass (chl *a*) (C, F) for Caillou Lake (A – C) and Barataria Bay (D – F) microcosm treatments over the course of the incubation. Error bars represent one standard deviation ($n = 3$). Shaded boxes (E, F) indicate f/40 nutrient additions.

percent diatoms and increased in percent cyanobacteria. The CL [1000] ppm cultures also began to decrease in percent diatoms, though the trend was more gradual, as they had not achieved as high a maximum during intermediate phase. All 6 cultures decreased or plateaued in C:N ratio. Finally, after 16 weeks of incubation, the treatments were dominated by filamentous cyanobacteria (10^7 to 10^8 cells L^{-1}). One notable deviation was in a [400] ppm replicate, which was the only culture to remain dominated by diatoms, experiencing a bloom of *C. simplex* (10^7 cells L^{-1}) and maintaining a presence of *Navicula* sp. (2×10^5 cells L^{-1}) (Fig. 5 A) (Supplementary Table 8). While *C. closterium* disappeared from all [400] ppm cultures, it persisted in 2 out of 3 [1000] ppm cultures in lesser amounts (10^4 , 10^5 cells L^{-1}) (Supplementary Table 9). The C:N ratio ranged between 6.9 and 8.5 in [400] ppm cultures and 5.1–7.3 in [1000] ppm cultures.

3.4. Barataria Bay

Assemblages from BB began shifting after 4 days (Fig. 4 C, D) with an increase in diatom populations, while cyanobacteria and dinoflagellates decreased and chlorophytes stayed constant (Fig. 4). This trend continued over the next 4 weeks of incubation as diatoms assemblages increased from 35% to 68–85% in 5 out of 6 Barataria Bay assemblages (Fig. 6).

Between week 4 and week 8, BB [400] ppm cultures decreased slightly to 60–75% diatoms (Fig. 6 A, C), while all BB [1000] ppm

cultures continued increasing, achieving a higher total percent diatoms of 90–95% (Fig. 6 D, F). Microscopic observation indicated diatom blooms were dominated by *C. closterium* in both [400] ppm cultures (10^4 – 10^7 cells L^{-1}) (Supplementary Table 10) and [1000] ppm cultures (10^6 – 10^7 cells L^{-1}) (Supplementary Table 11). Diatom blooms in both control and elevated pCO_2 treatment were also comprised of *Navicula* spp. (10^4 – 10^5 cells L^{-1}) (Supplementary Tables 9 & 10). Large *C. closterium* cells also developed in another BB [1000] ppm replicate. Two BB [1000] ppm treatments reached C:N peaks of 12 and 18 (Fig. 6 D, F), while all other cultures remained in the range of 5–10 for the entire incubation.

By the conclusion of the 16-week incubation period, the majority of the treatments remained dominated by diatoms (Fig. 6), a mix of chain forming diatoms (10^7 – 10^8 cells L^{-1}) and small pennate *Navicula* sp. (10^4 – 10^6 cells L^{-1}). While *C. closterium* persisted (10^4 – 10^5 cells L^{-1}) in [1000] ppm treatments at terminal sampling (Supplementary Table 11). The third [1000] ppm replicate showed 80% dominance by dinoflagellates at the terminal phase (Fig. 6, F). While an increased presence of *Karenia mikimotoi* was noted under the microscope (measuring 7.3×10^4 cells L^{-1}) (Supplementary Table 11), it is likely that the total biomass in this replicate was too low to give an accurate representation of the taxonomic composition via pigment analysis.

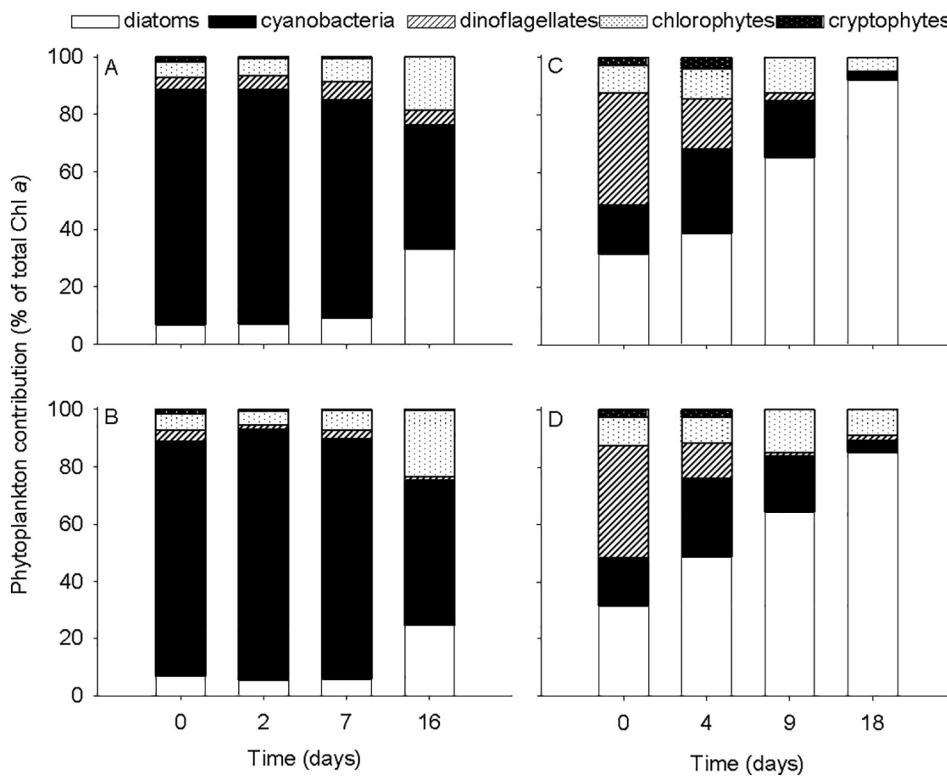


Fig. 4. Initial composition of diatoms (white), cyanobacteria (black), dinoflagellates (diagonal lines), chlorophytes (white with black dots) and cryptophytes (black with white dots) over the first two weeks; for (A) Caillou Lake [400] ppm, (B) Caillou Lake [1000] ppm, (C) Barataria Bay [400] ppm, and (D) Barataria Bay [1000] ppm microcosms treatments. Percent contribution bars represent an average ($n = 3$).

3.5. MDS Plots

For CL, [400] ppm treatment cultures were more likely to resemble the startup assemblages at the intermediate phase, while [1000] ppm treatment cultures were more likely to resemble startup assemblages at terminal sampling, while BB yielded different results (supplementary Fig. 1). Not all of the startup assemblages were within 80% similarity, which is likely due to the 4 day lag time between field collection and the official commencement of the incubation. For BB, terminal assemblages were more similar to startup assemblages than intermediate phases, with no distinction between pCO_2 treatments.

4. Discussion

Minute spatial variations mean there is no uniform pattern for phytoplankton community structure among estuaries. Estuaries habitually fluctuate across a wide range of physiochemical parameters, but anthropogenic influence may shift the boundary conditions. When combined with eutrophication or warming sea surface temperature, elevated pCO_2 may drive estuaries to experience more frequent and intense pH extremes, changing taxonomic composition by giving a competitive advantage of phytoplankton that thrive under those specific conditions (Hinga, 2002). This is difficult to predict, because the responses of species within a major taxonomic class vary. In creating a long-term data set, the importance of extended phytoplankton studies becomes apparent. For example, Nielsen et al. (2010) noted a lack of response of coastal plankton communities to increased free CO_2 and low pH after 14 days. They prescribed the nonresponse to the large diurnal and seasonal pH fluctuations typical of their study site, which may have created pH-tolerant algal species. This study indicates that 10 to 14-day sampling periods may not have been long enough in which to observe a response. After the initial two weeks of incubation, a pH difference had already been established in [400] and [1000] ppm Caillou Lake and Barataria Bay cultures, yet there was virtually no difference in the community structure between treatments in either estuarine assemblage. Although, it should be noted that the process of

screening through the 80 μm mesh to eliminate zooplankton likely also excluded larger diatoms and dinoflagellates, preventing their initial presence in phytoplankton assemblages for use in experimental incubation.

In this study, natural phytoplankton assemblages exposed to elevated pCO_2 experienced multiple transitional states over the course of a 16-week incubation with no direct successional path, demonstrating similar results to other natural community long-term mesocosm studies (Bach et al., 2016; Bach et al., 2017; Eberlein et al., 2017; Rasconi et al., 2017). Sampling occurred during the fall, a period of low river flow with primary production supported by storm-driven nutrient re-suspension. Caillou Lake is part of the prograding Atchafalaya deltaic system, with 98% of its freshwater coming from the river (Denes and Bayley, 1983). As river input peaks in spring and is at a minimum in fall, the water chemistry varies seasonally. In early fall, CL had a salinity of 12, indicating above average precipitation made up for the seasonal river discharge minimum (NOAA National Climate Report). Drainage from the surrounding tributaries after the flooding event in Louisiana in August 2016 probably also contributed to the low salinity (Watson et al., 2017). Barataria Bay is a degrading delta in the Mississippi River Plume, which receives relatively little riverine input. Water chemistry in lower Barataria is more driven by tides and gulf water levels than seasonality (Madden et al., 1988), and is consequently a more brackish and stable environment. In Caillou Lake and Barataria Bay, nitrates were below detection and phosphates were nearly equal. Barataria had double the ammonium concentration of Caillou Lake. These physiochemical factors played a role dictating the unique structure of the initial phytoplankton assemblage.

Each taxonomic class of phytoplankton varies in their competitive capabilities and ecological role, so community structure is not fixed, even in a particular area. Diatoms tend to dominate when silica is abundant (Officer and Ryther, 1980), and their large cell size make them particularly efficient in the process of sequestering carbon (Allen et al., 2005). Interestingly, though BB had half the amount of dissolved silica as CL, it had over twice the chl a or total biomass, assuming chl a as a proxy for phytoplankton biomass, and three times the relative

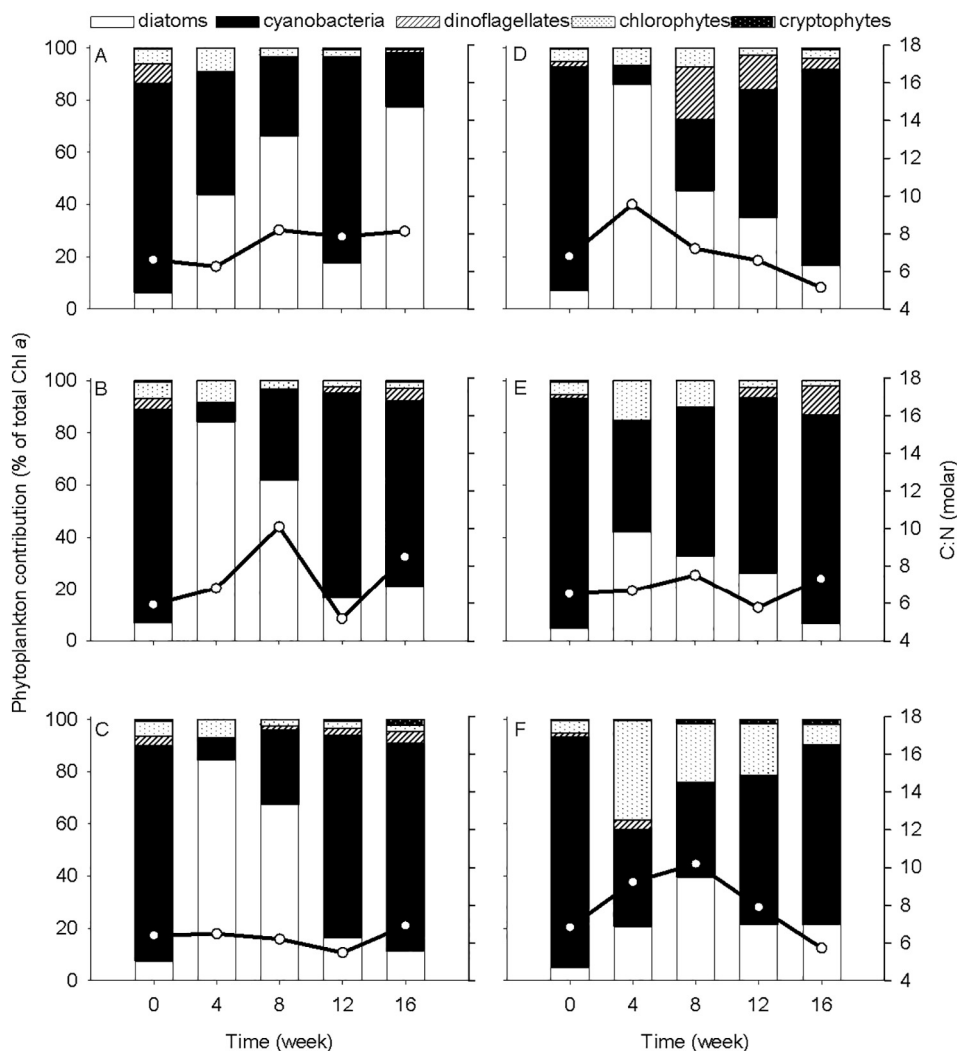


Fig. 5. Bars represent composition of diatoms (white), cyanobacteria (black), dinoflagellates (diagonal lines), chlorophytes (white with black dots) and cryptophytes (black with white dots) for individual microcosms from Caillou Lake over the course of the incubation, (A-C) $p\text{CO}_2$ [400] and (D-F) $p\text{CO}_2$ [1000]. Lines represent C:N molar ratios.

percent diatoms. However, DIN was below detection at both sites. Cyanobacteria often possess the ability to fix atmospheric nitrogen, and are not thus uninhibited by its absence (Allen and Arnon, 1955). In this situation, it's likely that Caillou Lake was nitrogen-limited, promoting cyanobacterial dominance (80%) over the expected diatoms. Barataria Bay was a rich mix of diatoms (31%), cyanobacteria (17%), and dinoflagellates (39%). Dinoflagellates are not great competitors for inorganic nutrients (Smayda and Reynolds, 2003), but many consume both organic and inorganic nutrients to make up for this (Litchman and Klausmeier, 2008; Smayda, 1997), perhaps giving them an advantage in the Barataria Bay field assemblage.

The focus of this experiment was observing a community-level response to different inorganic carbonate systems. The $p\text{CO}_2$ manipulation was successful in generating distinct pH values between treatments. It should be noted that startup cultures were at a pH of 8.5–8.7, near the upper end of the normal range reported from field studies (Guo et al., 2012). Four 14 weeks, [1000] ppm (elevated $p\text{CO}_2$) treatments remained within the range of pH 8 to pH 9, while [400] ppm (control) cultures rose from 9 to 10. Rising pH over the course of the experiment was also observed in previous microcosm studies (Engel et al., 2005), indicating that the inorganic carbon chemistry is influenced by more than just the introduction of $p\text{CO}_2$ enriched air via bubbling. Though it should be noted, that although the pH rose in both treatments, active bubbling of CO_2 occurred throughout the 16 weeks increasing the

availability of CO_2 to phytoplankton communities in the [1000] $p\text{CO}_2$ treatments. It was expected that as biological activity would influence the pH of the water, resulting from the conversion of inorganic carbon to an organic form during photosynthesis, but no significant relationship between the pH of the water and the biomass of phytoplankton cultures was observed during our experiments. The factors contributing to rising pH over time are still poorly understood, but may be attributed to nutrient levels and bacterial activity (Peixoto et al., 2013), which were not a focus of the current study.

Taxa vary in their physiological acquisition of inorganic carbon through use of a carbon concentrating mechanism (CCM), which uptakes HCO_3^- (Tortell et al., 2000). Regulation of the CCM is also dependent on the availability of light, nutrients, and trace metals (Raven and Johnston, 1991). As CO_2 and HCO_3^- are the main sources of inorganic carbon for phytoplankton, carbon may sometimes be a limiting nutrient (Riebesell et al., 1993). The converse of this concept suggests that elevated $p\text{CO}_2$ would encourage an increase in algal biomass, and is supported by recent studies showing enhanced overall biomass and primary production in acidified phytoplankton communities (Sommer et al., 2017; Taucher et al., 2017). However, in this study $p\text{CO}_2$ had no positive effect on the biomass of Caillou Lake or Barataria Bay cultures. Other research observed similar results in which elevated $p\text{CO}_2$ incited no significant change in gross primary production, net community production, particulate and dissolved carbon production, or growth

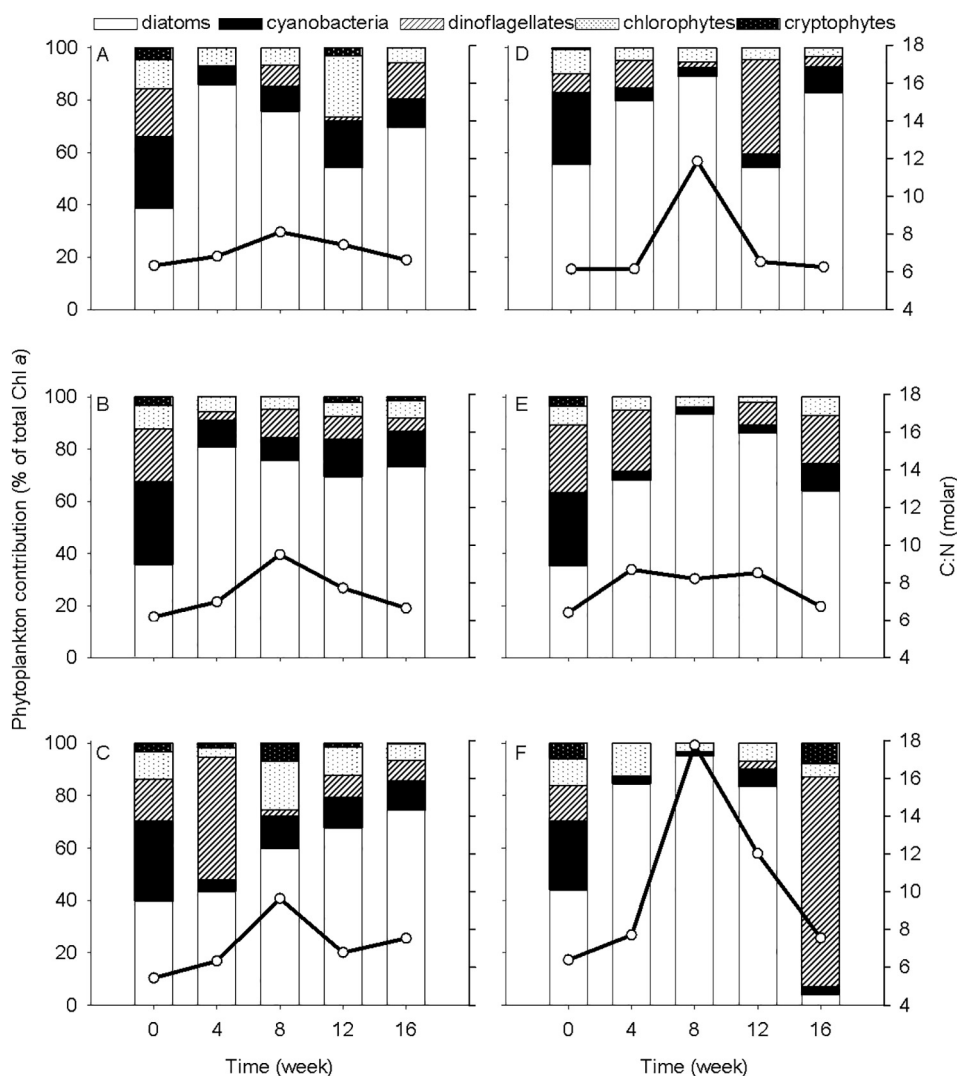


Fig. 6. Bars represent composition of diatoms (white), cyanobacteria (black), dinoflagellates (diagonal lines), chlorophytes (white with black dots) and cryptophytes (black with white dots) for individual microcosms from Barataria Bay over the course of the incubation, (A-C) $p\text{CO}_2$ [400] and (D-F) $p\text{CO}_2$ [1000]. Lines represent C:N molar ratios.

rates (Maugendre et al., 2015; Tortell et al., 2002). It seems that elevated $p\text{CO}_2$ does not implicitly catalyze an increase in phytoplankton biomass, contradicting the generalization that increased available carbon will drive algal blooms. Though it should be noted that the system was highly buffered, which may contribute to the lack of significant changes due to increased $p\text{CO}_2$.

Measure of biomass alone doesn't account for changes in species composition. CO_2 -driven shifts in the taxonomic structure of phytoplankton assemblages may occur without notable change to total primary productivity or biomass (Tortell et al., 2002). In this study, control cultures of Caillou Lake had a higher biomass than acidified treatments at times, while there was no difference in Barataria Bay cultures. This suggests changes in biomass may be a function of species-specific responses within the different startup communities. Monthly $f/40$ nutrient additions over the course of the 16-week incubation changed the availability of critical nutrients (N, P, and Si) as well as trace elements (Fe, Ni, Cu) (see supplementary material). This created a different competitive dynamic during incubation than would have been experienced in the field at the time of collection, and likely played a role dictating community structure.

In theory, changes in the relative contribution of major taxonomic groups should be more important in terms of ecological and biogeochemical function than genus or species levels shifts. However,

individual species can also play unique roles in their communities. While pigment data alone showcased a parabolic trend that made it appear that the assemblages returned to their startup community after 16 weeks of incubation, microscopic observations reveals this may not entirely be the case. For example, Caillou Lake assemblages were initially comprised of a diverse mixture of cyanobacteria, including *Microcystis*, *Anabaena*, *Cylindrospermopsis*, and *Raphidiopsis*. Intermediate assemblages, while greatly decreased in the total percent cyanobacteria due to diatoms blooms, contained similar cyanobacterial diversity. The total percent cyanobacteria increased again such that terminal assemblages contained a similar relative biovolume of cyanobacteria to the startup community. However, it was comprised of a singular species of filamentous cyanobacteria.

Even considering only taxonomic class, past community studies show variable and often conflicting responses to elevated $p\text{CO}_2$. For example, several species of chlorophytes increased at increased $p\text{CO}_2$ (Yang and Gao, 2003), or are favored over cyanobacteria and diatoms in a community setting (Low-Décarie et al., 2011; Gear et al., 2017; Taucher et al., 2017). However, Verschoor et al. (2013) found that cyanobacteria benefitted over chlorophytes while Bermúdez et al. (2016) noted that chlorophytes decreased overall at elevated $p\text{CO}_2$. In this study, an increase in chlorophytes was observed in one CL [1000] replicate after 4 weeks of incubation, but no distinctive response was

seen in any of the other elevated $p\text{CO}_2$ treatments. In another instance, Eggers et al. (2014) found that increased CO_2 selected for large diatoms like *Chaetoceros* sp. and *Thalassiosira constricta*. While these species were present in the Barataria Bay startup community, they disappeared in both BB [400] and BB [1000] ppm treatments. Nonetheless, all Barataria Bay elevated $p\text{CO}_2$ treatments did achieve higher diatom maxima than the controls (Fig. 6).

One diatom species, *Cylindrotheca cloisterum*, bloomed in all treatments and may have been impacted by increased $p\text{CO}_2$. The concentration of *C. cloisterum* was $7 \times 10^6 \pm 1.2 \times 10^7$ cells L^{-1} in [400] ppm cultures and $1.74 \times 10^7 \pm 2.95 \times 10^7$ cells L^{-1} in [1000] ppm treatments at intermediate sampling points. Unusually large, misshapen cells were observed in two [1000] ppm cultures, one from Caillou Lake and the other Barataria Bay. Their unique appearance may be attributed to an increase in the secretion of mucilage, which attracted agglomerations of small ($< 2 \mu\text{m}$) algae. This phenomenon was observed in response to a different stressor; Najdek et al. (2005) found that intrusions of high salinity water caused hyperproduction of mucilage in *C. cloisterum* cells. *C. cloisterum* has been known to thrive in nutrient-unbalanced systems (Alcoverro et al., 2000), such as the N limited/ Si abundant microcosm setup created during this incubation. It can maintain a competitive advantage under a range of pH values; in a community study (Pedersen and Hansen, 2003) found that in water of pH 8–8.5, 3 species of diatoms were numerous (*C. cloisterum*, *Cerataulina pelagica*, and *Leptocylindrus minimus*), but only *C. cloisterum* was present at pH 9–9.5. The pH of the [400] ppm cultures was in the same range, from 9.1 to 9.6, at the time of intermediate sampling. While *C. cloisterum* disappeared from [400] ppm assemblages in both Caillou Lake and Barataria Bay, it persisted (though at a decreased number, 10^4 – 10^5) in most of the [1000] ppm assemblages. At terminal sampling the pH ranged from 9.4–10.3 in control cultures and 9.1–10.1 in elevated $p\text{CO}_2$ cultures. The control cultures may have reached a pH above the tolerance range for this species.

Phytoplankton play an important role supplying energy to higher trophic levels, and changes in taxonomic composition may impact their nutritional value. The C:N ratio gives insight into metabolic activity and nitrogen uptake, and may have biogeochemical implications. Riebesell et al. (2007) found that C:N ratios at low CO_2 were comparable to the Redfield ratio (6.6), while at high CO_2 they rose to 8.0. In our study, notable C:N spikes of 12 and 18 were observed in two BB [1000] ppm cultures. As a general trend both [400] ppm and [1000] ppm cultures from Caillou Lake and Barataria Bay experienced intermediate maxima of C:N 8–10 before decreasing to startup values (6–7) by the terminal sampling period. Other research shows C:N varies in response to $p\text{CO}_2$, though not uniformly between species (Burkhardt et al., 1999; Tortell, 2000). Since different phytoplankton taxa are characterized by different stoichiometry under nutrient-replete conditions (Geider and La Roche, 2002), in this case C:N may have a relationship to diatom abundance, as they both achieve intermediate maxima. Higher C:N ratios would increase the magnitude of carbon sequestration and could prove to be a negative feedback mechanism balancing increasing atmospheric $p\text{CO}_2$. However, high C:N is also indicative of nutrient limitation, and a lower C:N ratio may also be indicative of better nutritional value available to primary consumers. The role that $p\text{CO}_2$ plays in the elemental composition of phytoplankton, and its deviation from the Redfield ratio, should continue to be a priority in new research.

An interesting feedback loop to consider is the relationship between phytoplankton and trace metal concentrations at elevated $p\text{CO}_2$. Not only does the abundance of trace metals influence productivity and species composition of phytoplankton communities, but the algae also control the distribution of trace metals (Sunda, 2012). The pH of seawater may alter the chemical speciation and dissolved concentrations of certain metals, like copper (Graneli and Haraldsson, 1993; Kester, 1986). Likewise, acidification has been shown to decrease the rate of iron uptake in diatoms and coccolithophores (Shi et al., 2010). Higher amount of certain trace elements (Ni, Cu, Cd, Co) were observed in

[1000] ppm BB cultures than [400] ppm cultures (supplementary Fig. 2), despite having comparable biomass and warrants further study.

Nutrients were added after 2 weeks, and by week 4 of incubation each assemblage had diverged in taxonomic composition. At the intermediate sampling period (week 8), Caillou Lake and Barataria Bay observed opposite responses between their [400] ppm and [1000] ppm cultures. For example, in Caillou Lake assemblages, all three [400] ppm replicates had similar taxonomic structures (60% diatoms, 30% cyanobacteria, 0.5% dinoflagellates, 3% chlorophytes), while [1000] ppm replicates saw individual increases in dinoflagellates (to 20%) or chlorophytes (10%, 23%). Even though the cultures were different at 8 weeks, by terminal sampling the majority had returned to their startup compositions, dominated by cyanobacteria in Caillou Lake and diatoms in Barataria Bay. This return to the initial community structure was only observed after 14–16 weeks of incubation, indicating that phytoplankton may show evidence of adaptive evolution to elevated $p\text{CO}_2$ exposure during long term experiments.

Future studies should continue to explore the synergistic effect of low pH and other environmental variables such as nutrients, salinity, and temperature. While certain areas, like coastal Louisiana, may be accustomed to acute low pH exposure, elevated $p\text{CO}_2$ could increase sensitivity towards other environmental factors. Growth and community composition have been shown to be jointly affected by $p\text{CO}_2$ and nutrient addition (Low-Décarie et al., 2015), but elevated temperature may be a stronger driver of community composition than acidification (Hare et al., 2007; Sommer et al., 2015). Results from short-term or single-factor studies may not necessarily be representative of phytoplankton response in the long term. In the longest study reviewed, Rasconi et al. (2017) found that over the course of an 8 month incubation, elevated and fluctuating temperature resulted in lower growth of larger species, also decreasing diversity and evenness as cyanobacteria and chlorophytes gained dominance. Extending the length of incubation experiments and incorporating multiple factors allows for more comprehensive predictions for life in a changing climate.

5. Conclusions

The physiochemical factors and initial phytoplankton community structure in Caillou Lake and Barataria Bay was fundamental to our results. The phytoplankton community collected from Caillou Lake was dominated by an assortment of cyanobacteria, while Barataria Bay was an even more diverse mixture of diatoms, dinoflagellates, cyanobacteria, and nanoflagellates. Over the first week of incubation, the taxonomic structure of all Caillou Lake assemblages was unchanged. In contrast, Barataria Bay assemblages began changing after only four days. Over the course of the 16-week incubation, [400] ppm and [1000] ppm treatments in both Caillou Lake and Barataria Bay assemblages followed the same general parabolic successional pattern. Over the first 4–8 weeks they increased in relative percent diatoms, reaching a maximum at the intermediate stage, and then from weeks 8 to 16 transitioned to the startup community structure. By the end of the 16-week incubation, 10 out of the 12 cultures had a community structure analogous to that of the startup phytoplankton assemblage collected from the field. This finding supports conclusions by Eggers et al. (2014), who suggest that the initial ratio between major taxonomic classes is the main driver behind community structure, even at different pH levels. This trend suggests adaptation and competition was observed due to the long-term incubation (16-weeks). Our results highlight the need for long-term, community level microcosm studies, indicating that there was no deterministic response in biomass, community structure, or C:N dictated by elevated $p\text{CO}_2$. On the contrary, comparison between different startup communities and past studies suggests that results from one area may not be generalized to other coastal ecosystems. Thus, current climate change models amalgamating response to increased $p\text{CO}_2$ by plankton functional types may not truly be representative.

Acknowledgements

This work has been supported with funding provided by the Louisiana Sea Grant College Program (LSG) under NOAA Award # NA14OAR4170099. The funding support of LSG and NOAA is gratefully acknowledged. We thank Darian Madere (LSU), Jace Hood (LSU), Tiffany Pasco (LSU), and Steven Madere (LSU) for their technical assistance during the experiments and in the field.

Appendix A. Supplementary data

Supplementary data to this article can be found online at <https://doi.org/10.1016/j.jembe.2018.09.008>.

References

- Alcoverro, T., Conte, E., Mazzella, L., 2000. Production of mucilage by the Adriatic epipelagic diatom *Cylindrotheca closterium* (Bacillariophyceae) under nutrient limitation. *J. Phycol.* 36 (6), 1087–1095.
- Allen, M.B., Arnon, D.I., 1955. Studies on nitrogen-fixing blue-green algae. I. Growth and nitrogen fixation by *Anabaena cylindrica* Lemm. *Plant Physiol.* 30 (4), 366.
- Allen, J.T., Brown, L., Sanders, R., Moore, C.M., Mustard, A., Fielding, S., Lucas, M., Rixen, M., Savidge, G., Henson, S., 2005. Diatom carbon export enhanced by silicate upwelling in the Northeast Atlantic. *Nature* 437 (7059), 728–732.
- Bach, L.T., Taucher, J., Boxhammer, T., Ludwig, A., Achterburg, E.P., Aluero-Muñiz, A., Anderson, L.G., Bellworthy, J., Biedenbender, J., Czerny, J., Ericson, Y., Esposito, M., Fischer, M., Haunost, M., Hellemann, D., Horn, H.G., Hornick, T., Meyer, J., Sswat, M., Zark, M., Riebesell, U., 2016. Influence of ocean acidification on a natural winter-to-summer plankton succession: first insights from a long-term mesocosm study draw attention to periods of low nutrient concentrations. *PLoS ONE* 11 (8), e0159068.
- Bach, L.T., Alvarez-Fernandez, S., Hornick, T., Stühr, A., Riebesell, U., 2017. Simulated ocean acidification reveals winners and losers in coastal phytoplankton. *PLoS ONE* 12 (11), e0188198.
- Beardall, J., Ihnken, S., Quigg, A., 2009. Gross and net primary production: closing the gap between concepts and measurements. *Aquat. Microb. Ecol.* 56, 113–122.
- Bermúdez, R., Winder, M., Stühr, A., Almén, A.-K., Engström-Öst, J., Riebesell, U., 2016. Effect of ocean acidification on the structure and fatty acid composition of a natural plankton community in the Baltic Sea. *Biogeosciences* 13 (24), 6625.
- Bianchi, T.S., Pennock, J.R., Twilley, R.R., 1999. Biogeochemistry of Gulf of Mexico Estuaries: John Wiley and Sons. US, New Jersey.
- Bockmon, E.E., Dickson, A.G., 2014. A seawater filtration method suitable for total dissolved inorganic carbon and pH analyses. *Limnol. Oceanogr.* 12, 191–195.
- Borges, A.V., Gypens, N., 2010. Carbonate chemistry in the coastal zone responds more strongly to eutrophication than ocean acidification. *Limnol. Oceanogr.* 55 (1), 346–353.
- Burkhardt, S., Zondervan, I., Riebesell, U., 1999. Effect of CO₂ concentration on C:N:P ratio in marine phytoplankton: a species comparison. *Limnol. Oceanogr.* 44 (3), 683–690.
- Cai, W.-J., 2003. Riverine inorganic carbon flux and rate of biological uptake in the Mississippi River plume. *Geophys. Res. Lett.* 30 (2).
- Cai, W.-J., Hu, X., Huang, W.-J., Jiang, L.-Q., Wang, Y., Peng, T.H., Zhang, X., 2010. Alkalinity distribution in the western North Atlantic Ocean margins. *J. Geophys. Res.* 115 (C8).
- Cai, W.-J., Hu, X., Huang, W.-J., Murrell, M.C., Lehrter, J.C., Lohrenz, S.E., Chou, W.-C., Zhai, W., Hollibaugh, J.T., Wang, Y., 2011. Acidification of subsurface coastal waters enhanced by eutrophication. *Nat. Geosci.* 4 (11), 766–770.
- Caldeira, K., Wickett, M.E., 2003. Oceanography: anthropogenic carbon and ocean pH. *Nature* 425 (6956), 365.
- Collins, S., Rost, B., Rynearson, T.A., 2014. Evolutionary potential of marine phytoplankton under ocean acidification. *Evol. Appl.* 7 (1), 140–155.
- Dai, M., Zhai, W., Cai, W.-J., Callahan, J., Huang, B., Shang, S., Huang, T., Li, X., Lu, Z., Chen, W., 2008. Effects of an estuarine plume-associated bloom on the carbonate system in the lower reaches of the Pearl River estuary and the coastal zone of the northern South China Sea. *Cont. Shelf Res.* 28 (12), 1416–1423.
- D'Elia, C.F., 1977. The uptake and release of dissolved phosphorus by reef corals 1, 2. *Limnol. Oceanogr.* 22, 301–315.
- Dickson, A.G., 1990. Standard potential of the reaction: AgCl (s) + 12H₂O (g) = Ag (s) + HCl (aq), and the standard acidity constant of the ion HSO⁻4 in synthetic sea water from 273.15 to 318.15 K. *J. Chem. Thermodyn.* 22 (2), 113–127.
- Dickson, A., Millero, F.J., 1987. A comparison of the equilibrium constants for the dissociation of carbonic acid in seawater media. *Deep Sea Res. Part 1 Oceanogr. Pap.* 34 (10), 1733–1743.
- Dickson, A.G., Sabine, C.L., Christian, J.R. (Eds.), 2007. Guide to best practices for ocean CO₂ measurements, PICES Special Publication. Vol. 3 North Pacific Marine Science Organization, BC, Canada.
- Dutkiewicz, S., Morris, J.J., Follows, M.J., Scott, J., Levitan, O., Dyhrman, S.T., Berman-Frank, I., 2015. Impact of ocean acidification on the structure of future phytoplankton communities. *Nat. Clim. Chang.* 5 (11), 1002–1006.
- Eberlein, T., Wohlrab, S., Rost, B., Uwe, J., Bach, L.T., Riebesell, U., Van de Waal, D.B., 2017. Effects of ocean acidification on primary production in a coastal North Sea phytoplankton community. *PLoS ONE* 12 (3), e0172594.
- Eggers, S.L., Lewandowska, A.M., Barcelos E Ramos, J., Blanco-Ameijeiras, S., Gallo, F., Matthiessen, B., 2014. Community composition has greater impact on the functioning of marine phytoplankton communities than ocean acidification. *Glob. Chang. Biol.* 20 (3), 713–723.
- Engel, A., Zondervan, I., Aerts, K., Beaufort, L., Benthien, A., Chou, L., Delille, B., Gattuso, J.-P., Harlay, J., Heemann, C., 2005. Testing the direct effect of CO₂ concentration on a bloom of the coccolithophorid *Emiliania huxleyi* in mesocosm experiments. *Limnol. Oceanogr.* 50 (2), 493–507.
- Feely, R.A., Sabine, C.L., Lee, K., Berelson, W., Kleypas, J., Fabry, V.J., Millero, F.J., 2004. Impact of anthropogenic CO₂ on the CaCO₃ system in the oceans. *Science* 305 (5682), 362–366.
- French, R.H., Watts, R.J., 1989. Performance of in-situ microcosms compared to actual reservoir behavior. *J. Environ. Eng.* 115 (4), 835–849.
- Geider, R., La Roche, J., 2002. Redfield revisited: variability of C:N:P in marine microalgae and its biochemical basis. *Eur. J. Phycol.* 37 (1), 1–17.
- Graneli, E., Haraldsson, C., 1993. Can Increased Leaching of Trace Metals from Acidified Areas Influence Phytoplankton Growth in Coastal Waters? *Ambio*. pp. 308–311.
- Guo, X., Cai, W.-J., Huang, W.-J., Wang, Y., Chen, F., Murrell, M.C., Lohrenz, S.E., Jiang, L.-Q., Dai, M., Hartmann, J., 2012. Carbon dynamics and community production in the Mississippi River plume. *Limnol. Oceanogr.* 57 (1), 1–17.
- Hare, C.E., Leblanc, K., Ditullio, G.R., Kudela, R.M., Zhang, Y., Lee, P.A., Riseman, S., Hutchins, D.A., 2007. Consequences of increased temperature and CO₂ for phytoplankton community structure in the Bering Sea. *Mar. Ecol. Prog. Ser.* 352, 9–16.
- Haukka, K., Kolmonen, E., Hyder, R., Hietala, J., Vakkilainen, K., Kairesalo, T., Haario, H., Sivonen, K., 2006. Effect of nutrient loading on bacterioplankton community composition in lake mesocosms. *Microb. Ecol.* 51, 137–146.
- Hein, M., Sand-Jensen, K., 1997. CO₂ increases oceanic primary production. *Nature* 388, 526–527.
- Hettinger, A., Sanford, E., Hill, T.M., Hosfelt, J.D., Russell, A.D., Gaylord, B., 2013. The influence of food supply on the response of Olympia oyster larvae to ocean acidification. *Biogeosciences* 10 (10), 6629–6638.
- Hinga, K.R., 2002. Effects of pH on coastal marine phytoplankton. *Mar. Ecol. Prog. Ser.* 238, 281–300.
- Hondzo, M., Lyn, D., 1999. Quantified small-scale turbulence inhibits the growth of a green alga. *Freshw. Biol.* 41 (1), 51–61.
- IPCC, 2013. Climate Change 2013: The Physical Science Basis. In: Stocker, T.F., Qin, D., Plattner, G.-K., Tignor, M., Allen, S.K., Boschung, J., Nauels, A., Xia, Y., Bex, V., Midgley, P.M. (Eds.), Contribution of Working Group I to the Fifth Assessment Report of the Intergovernmental Panel on Climate Change. Cambridge University Press, Cambridge.
- Juhl, A.R., Latz, M.I., 2002. Mechanisms of fluid shear-induced inhibition of population growth in a red-tide dinoflagellate. *J. Phycol.* 38 (4), 683–694.
- Kester, D., 1986. Equilibrium models in seawater: Applications and limitations. In: Bernhard (Ed.), The Importance of Chemical “Speciation” in Environmental Processes. Springer, Berlin, Germany, pp. 337–363.
- Keul, N., Morse, J.W., Wanninkhof, R., Gledhill, D.K., Bianchi, T.S., 2010. Carbonate chemistry dynamics of surface waters in the northern Gulf of Mexico. *Aquat. Geochem.* 16 (3), 337–351.
- Kim, J.-M., Lee, K., Shin, K., Kang, J.-H., Lee, H.-W., Kim, M., Jang, P.-G., Jang, M.-C., 2006. The effect of seawater CO₂ concentration on growth of a natural phytoplankton assemblage in a controlled mesocosm experiment. *Limnol. Oceanogr.* 51 (4), 1629–1636.
- Lewitus, A.J., White, D.L., Tymowski, R.G., Geesey, M.E., Hymel, S.N., Noble, P.A., 2005. Adapting the CHEMTAX method for assessing phytoplankton taxonomic composition in southeastern US estuaries. *Estuaries* 28 (1), 160–172.
- Litchman, E., Klausmeier, C.A., 2008. Trait-based community ecology of phytoplankton. *Annu. rev. Ecol. Syst.* 39, 615–639.
- Lohrenz, S.E., Cai, W.-J., 2006. Satellite Ocean color assessment of air-sea fluxes of CO₂ in a river-dominated coastal margin. *Geophys. Res. Lett.* 33 (1).
- Low-Décarie, E., Fussmann, G.F., Bell, G., 2011. The effect of elevated CO₂ on growth and competition in experimental phytoplankton communities. *Glob. Change Biol.* *Bioenergy* 17 (8), 2525–2535.
- Low-Décarie, E., Bell, G., Fussmann, G.F., 2015. CO₂ alters community composition and response to nutrient enrichment of freshwater phytoplankton. *Oecologia* 177 (3), 875–883.
- Mackey, M., Mackey, D., Higgins, H., Wright, S., 1996. CHEMTAX—a program for estimating class abundances from chemical markers: application to HPLC measurements of phytoplankton. *Mar. Ecol. Prog. Ser.* 144, 265–283.
- Madden, C.J., Day, J.W., Randall, J.M., 1988. Freshwater and marine coupling in estuaries of the Mississippi River deltaic plain. *Limnol. Oceanogr.* 33, 982–1004.
- Maugendre, L., Gattuso, J.-P., Poulton, A., Dellisanti, W., Gaubert, M., Guieu, C., Gazeau, F., 2015. No detectable effect of ocean acidification on plankton metabolism in the NW oligotrophic Mediterranean Sea: results from two mesocosm studies. *Estuar. Coast. Shelf Sci.* 186A, 89–99.
- Mehrbach, C., Culbertson, C.H., Hawley, J.E., Pytkowicz, R.M., 1973. Measurement of the apparent dissociation constants of carbonic acid in seawater at atmospheric pressure. *Limnol. Oceanogr.* 18 (6), 897–907.
- Monastersky, R., 2013. Global carbon dioxide levels near worrisome milestone. *Nature* 497 (7447), 13.
- Najdek, M., Blažina, M., Djakovac, T., Kraus, R., 2005. The role of the diatom *Cylindrotheca closterium* in a mucilage event in the northern Adriatic Sea: coupling with high salinity water intrusions. *J. Plankton Res.* 27 (9), 851–862.
- Nielsen, L.T., Jakobsen, H.H., Hansen, P.J., 2010. High resilience of two coastal plankton communities to twenty-first century seawater acidification: evidence from mesocosm studies. *Mar. Biol.* Res. 6 (6), 542–555.
- Nielsen, L.T., Hallegraeff, G.M., Wright, S.W., Hansen, P.J., 2012. Effects of experimental

- seawater acidification on an estuarine plankton community. *Aquat. Microb. Ecol.* 65 (3), 271–285.
- O'Dell, J., 1993a. Method 350.1: Determination of Ammonia Nitrogen by Semi-Automated Colorimetry Methods for the Determination of Inorganic Substances in Environmental Samples: EPA/600/R-93/100. US Environmental protection Agency.
- O'Dell, J.W., 1993b. Method 353.2, Revision 2.0: Determination of Nitrate-Nitrite Nitrogen by Automated Colorimetry. US Environmental protection Agency.
- O'Dell, J., 1993c. Determination of Phosphorus by Semi-Automated Colorimetry. Environmental monitoring systems laboratory office of research and development US. US Environmental protection Agency.
- Officer, C., Ryther, J., 1980. The possible importance of silicon in marine eutrophication. *Mar. Ecol. Prog. Ser.* 3 (1), 83–91.
- Orr, J.C., Fabry, V.J., Aumont, O., Bopp, L., Doney, S.C., Feely, R.A., Gnanadesikan, A., Gruber, N., Ishida, A., Joos, F., 2005. Anthropogenic Ocean acidification over the twenty-first century and its impact on calcifying organisms. *Nature* 437 (7059), 681–686.
- Parsons, T., Malta, Y., Lalli, C., 1984. *A Manual of Chemical and Biological Methods for Seawater Analysis*. Pergamon Press, New York.
- Pearson, P.N., Palmer, M.R., 2000. Atmospheric carbon dioxide concentrations over the past 60 million years. *Nature* 406 (6797), 695–699.
- Pedersen, M.F., Hansen, P.J., 2003. Effects of high pH on a natural marine planktonic community. *Mar. Ecol. Prog. Ser.* 260, 19–31.
- Peixoto, R.B., Marotta, H., Enrich-Prast, A., 2013. Experimental evidence of nitrogen control on pCO₂ in phosphorus-enriched humid and clear coastal lagoon waters. *Front. Microbiol.* 4.
- Pierrot, D., Lewis, E., Wallace, D., 2006. MS Excel Program Developed for CO₂ System Calculations. Carbon Dioxide Information Analysis Center, Oak Ridge National Laboratory. US Department of Energy, *ORNL/CDIAC-105*.
- Pinckney, J., Paerl, H., Harrington, M., Howe, K., 1998. Annual cycles of phytoplankton community-structure and bloom dynamics in the Neuse River Estuary, North Carolina. *Mar. Bio.* 131 (2), 371–381.
- Rasconi, S., Winter, K., Kainz, M.J., 2017. Temperature increase and fluctuation induce phytoplankton biodiversity loss—evidence from a multi-seasonal mesocosm experiment. *Ecol. Evol.* 7 (9), 2936–2946.
- Raven, J.A., Johnston, A.M., 1991. Mechanisms of inorganic-carbon acquisition in marine phytoplankton and their implications for the use of other resources. *Limnol. Oceanogr.* 36 (8), 1701–1714.
- Raven, J., Caldeira, K., Elderfield, H., Hoegh-Guldberg, O., Liss, P., Riebesell, U., Shepherd, J., Turley, C., Watson, A., 2005. Ocean acidification due to increasing atmospheric carbon dioxide. The Royal Society policy document 12.05 Cardiff. Clyvedon Press, UK.
- Riebesell, U., Tortell, P.D., 2011. Effects of ocean acidification on pelagic organisms and ecosystems. In: Gattuso, J.P., Hansson, L. (Eds.), *Ocean Acidification*. Oxford University Press, Oxford, pp. 99–121.
- Riebesell, U., Wolf-Gladrow, D.A., Smetacek, V., 1993. Carbon dioxide limitation of marine phytoplankton growth rates. *Nature* 361, 249–251.
- Riebesell, U., Schulz, K.G., Bellerby, R., Botros, M., Fritsche, P., Meyerhöfer, M., Neill, C., Nondal, G., Oeschlies, A., Wohlers, J., 2007. Enhanced biological carbon consumption in a high CO₂ ocean. *Nature* 450 (7169), 545–548.
- Rossoll, D., Bermúdez, R., Hauss, H., Schulz, K.G., Riebesell, U., Sommer, U., Winder, M., 2012. Ocean acidification-induced food quality deterioration constrains trophic transfer. *PLoS ONE* 7 (4), e34737.
- Rost, B., Zondervan, I., Wolf-Gladrow, D., 2008. Sensitivity of phytoplankton to future changes in ocean carbonate chemistry: current knowledge, contradictions and research directions. *Mar. Ecol. Prog. Ser.* 373237, 227, 227–237.
- Sabine, C.L., Feely, R.A., Gruber, N., Key, R.M., Lee, K., Bullister, J.L., Wanninkhof, R., Wong, C., Wallace, D.W., Tilbrook, B., 2004. The oceanic sink for anthropogenic CO₂. *Science* 305 (5682), 367–371.
- Schippers, P., Lurling, M., Scheffer, M., 2004. Increase of atmospheric CO₂ promotes phytoplankton productivity. *Ecol. Lett.* 7 (6), 446–451.
- Sengupta, A., Carrara, F., Stocker, R., 2017. Phytoplankton can actively diversify their migration strategy in response to turbulent cues. *Nature* 543 (7646), 555–558.
- Shi, D., Xu, Y., Hopkinson, B.M., Morel, F.M.M., 2010. Effect of ocean acidification on iron availability to marine phytoplankton. *Science* 327 (5966), 676–679.
- Smayda, T.J., 1997. Harmful algal blooms: their ecophysiology and general relevance to phytoplankton blooms in the sea. *Limnol. Oceanogr.* 42, 1137–1153.
- Smayda, T.J., Reynolds, C.S., 2003. Strategies of marine dinoflagellate survival and some rules of assembly. *J. Sea Res.* 49 (2), 95–106.
- Solomon, S., Qin, D., Manning, M., Chen, Z., Marquis, M., Averyt, K.B., Tignor, M., Miller, H.L., 2007. Contribution of Working Group I to the Fourth Assessment Report of the Intergovernmental Panel on Climate Change Climate. Climate Change. The physical science basis. Cambridge University Press, Cambridge, pp. 2007.
- Sommer, U., 1985. Comparison between steady state and nonsteady state competition: experiments with natural phytoplankton. *Limnol. Oceanogr.* 30, 335–346.
- Sommer, U., Paul, C., Moustaka-Gouni, M., 2015. Warming and ocean acidification effects on phytoplankton—from species shifts to size shifts within species in a mesocosm experiment. *PLoS ONE* 10 (5), e0125239.
- Sommer, U., Peter, K.H., Genitsaris, S., Moustaka-Gouni, M., 2017. Do marine phytoplankton follow Bergmann's rule sensu lato? *Bio. Rev.* 92 (2), 1011–1026.
- Sullivan, J.M., Swift, E., Donaghay, P.L., Rines, J.E.B., 2003. Small-scale turbulence affects the division rate and morphology of two red-tide dinoflagellates. *Harmful Algae* 2 (3), 183–199.
- Sun, J., Liu, D., 2003. Geometric models for calculating cell biovolume and surface area for phytoplankton. *J. Plankton Res.* 25 (11), 1331–1346.
- Sunda, W., 2012. Feedback interactions between trace metal nutrients and phytoplankton in the ocean. *Front. Microbiol.* 3, 204.
- Sunda, W.G., Cai, W.-J., 2012. Eutrophication Induced CO₂-Acidification of Subsurface Coastal Waters: Interactive Effects of Temperature, Salinity, and Atmospheric pCO₂. *Environ. Sci. Technol.* 46 (19), 10651–10659.
- Tagliabue, A., Bopp, L., Gehlen, M., 2011. The response of marine carbon and nutrient cycles to ocean acidification: large uncertainties related to phytoplankton physiological assumptions. *Glob. Biogeochem. Cycles* 25 (3).
- Taucher, J., Oeschlies, A., 2011. Can we predict the direction of marine primary production change under global warming? *Geophys. Res. Lett.* 38 (2).
- Taucher, J., Haunost, M., Boxhammer, T., Bach, L.T., Algueró-Muñoz, M., Riebesell, U., 2017. Influence of ocean acidification on plankton community structure during a winter-to-summer succession: an imaging approach indicates that copepods can benefit from elevated CO₂ via indirect food web effects. *PLoS ONE* 12 (2), e0169737.
- Tortell, P.D., 2000. Evolutionary and ecological perspectives on carbon acquisition in phytoplankton. *Limnol. Oceanogr.* 45 (3), 744–750.
- Tortell, P.D., Rau, G.H., Morel, F.M., 2000. Inorganic carbon acquisition in coastal Pacific phytoplankton communities. *Limnol. Oceanogr.* 45 (7), 1485–1500.
- Tortell, P.D., Ditullio, G.R., Sigman, D.M., Morel, F.M., 2002. CO₂ effects on taxonomic composition and nutrient utilization in an Equatorial Pacific phytoplankton assemblage. *Mar. Ecol. Prog. Ser.* 236, 37–43.
- Tortell, P.D., Payne, C.D., Li, Y., Trimborn, S., Rost, B., Smith, W.O., Riesselman, C., Dunbar, R.B., Sedwick, P., Ditullio, G.R., 2008. CO₂ sensitivity of Southern Ocean phytoplankton. *Geophys. Res. Lett.* 35 (4).
- Uppström, L.R., 1974. The boron/chlorinity ratio of deep-sea water from the Pacific Ocean. *Deep Sea Res. Oceanogr. Abst.* 21 (2), 161–162.
- Van Heukelem, L., Lewitus, A., Kana, T., Craft, N., 1995. Improved separations of phytoplankton pigments using temperature-controlled high performance liquid chromatography. *Oceanograph Lit. Rev.* 5 (42), 376.
- Verschoor, A.M., Van Dijk, M.A., Huisman, J., Van Donk, E., 2013. Elevated CO₂ concentrations affect the elemental stoichiometry and species composition of an experimental phytoplankton community. *Freshw. Biol.* 58 (3), 597–611.
- Wallace, R.B., Baumann, H., Grear, J.S., Aller, R.C., Gobler, C.J., 2014. Coastal Ocean acidification: the other eutrophication problem. *Estuar. Coast. Shelf Sci.* 148, 1–13.
- Wang, Z.A., Wanninkhof, R., Cai, W.-J., Byrne, R.H., Hu, X., Peng, T.-H., Huang, W.-J., 2013. The marine inorganic carbon system along the Gulf of Mexico and Atlantic coasts of the United States: Insights from a transregional coastal carbon study. *Limnol. Oceanogr.* 58 (1), 325–342.
- Wanninkhof, R., Barbero, L., Byrne, R., Cai, W.-J., Huang, W.-J., Zhang, J.-Z., Baringer, M., Langdon, C., 2015. Ocean acidification along the Gulf Coast and East Coast of the USA. *Cont. Shelf Res.* 98, 54–71.
- Watson, K.M., Storm, J.B., Breaker, B.K., Rose, C.E., 2017. Characterization of Peak Streamflows and Flood Inundation of Selected Areas in Louisiana from the August 2016 Flood: US Geological Survey.
- Wissel, B., Gaçe, A., Fry, B., 2005. Tracing river influences on phytoplankton dynamics in two Louisiana estuaries. *Ecology* 86 (10), 2751–2762.
- Xiao, Y., Li, Z., Li, C., Zhang, Z., Guo, J.S., 2016. Effect of small-scale turbulence on the physiology and morphology of two bloom-forming cyanobacteria. *PlosOne* 11 (12), e0168925.
- Yang, Y., Gao, K., 2003. Effects of CO₂ concentrations on the freshwater microalgae, *Chlamydomonas reinhardtii*, *Chlorella pyrenoidosa* and *Scenedesmus obliquus* (Chlorophyta). *J. Appl. Phycol.* 15 (5), 379–389.
- Zhao, Y., Quigg, A., 2014. Nutrient limitation in Northern Gulf of Mexico (NGOM): phytoplankton communities and photosynthesis respond to nutrient pulse. *PLoS ONE* 9 (2), e88732.
- Zimmermann, C., Keefe, C., Bashe, J., 1997. Method 449.9 Determination of Carbon and Nitrogen in Sediments and Particulates of Estuarine/Coastal Waters Using Elemental Analysis. US Environmental Protection Agency.